XLI CILAMCE
XLI Ibero-Latin American Congress on Computational Methods in Engineering
16-19 November, 2020 FOZ DO IGUAÇU PARANÁ - BRAZIL

Numerical analysis on the compression behavior of pultruded GFRP angle sections with bolted connections

Diniz A. C. M.[1], Malite M.[1]

[1]*Dept. of Structural Engineering, São Carlos School of Engineering, University of São Paulo*
Av. Trabalhador São Carlense - 400, 13566-590, São Carlos/São Paulo, Brazil

Abstract. This paper evaluates different strategies for simulating the compression behavior of 50×6 mm pultruded Glass Fiber Reinforced Polymer (pGFRP) angles with bolted connections. A brief review of the studies on pGFRP angles connected by the leg shows that the studies on the mechanical behavior of eccentrically loaded angles are still scarce. On the other hand, studies on steel angles have been developed for decades. Based on the methodology presented in recent works on steel angles bolted by the leg, some numerical modeling parameters, such as material and damage failure criteria, mesh size and shape, boundary and loading conditions, and others were evaluated and discussed. Finally, a shell Finite Element (FE) model was proposed in ABAQUS®. The theoretical critical loads predicted using FE were compared to analytical prediction obtained by Vlasov equation. Using the Hashin material damage model, progressive failure analyses were performed to simulate experimental tests with pGFRP angles eccentrically loaded by two bolts. Results have shown that the usual procedure adopted in works available in literature (neglecting eccentricity) does not provide an accurate estimate, moreover, non-linear buckling analyses provides satisfactory agreement between the proposed model and the experiments.

Keywords: Pultruded glass-fiber reinforced polymer, angles columns, buckling, numerical analyses.

1 Introduction

Over the past years, structures made of pultruded Glass Fiber Reinforced Polymers (pGFRP) have been adopted as a viable and efficient solution to civil engineering structural projects. Their use is specifically advantageous when light-strength and non-corrosive or electrically non-conductive structures are required. The unidirectional load-carrying behavior of pGFRP profiles make them particularly attractive in structures assembled with the use of two-force members, such roof structures, trusses, joists, and towers. Due to their simplicity and easiness for the creation of bolted connections, pGFRP angles are widely adopted as a member of this type of structure. As consequence, they are often found under eccentric compression caused by bolted connections along their legs. The eccentricity is induced due to non-coincidence of load transfer line with the centroidal line of bolted connection, so that the bar is subjected to combined efforts of compression and bending.

It is well known that the additional stresses originated due the bending moment affects the ultimate strength and stability of pGFRP angles. However, Galambos [1] highlights that when the load is introduced through bolted connections, an additional rigidity is given to the connection, partially restricting the bending and warping of the ends. So, it is be noted that the strength prediction of angles connected by the leg is not so trivial. In fact, to fully understand the influence of the load eccentricity and the additional stiffness provided by bolted connection on the mechanical behavior of the angles connected by the leg, these aspects need to be particularly investigated.

To date, the studies on the mechanical behavior of pGFRP angles bolted by the leg are still scarce and the current versions of design codes for GFRP composite structures do not provide recommendations for angles whose ends are connected by bolts. With a lower demand for resources than that required to carry out laboratory tests, numerical simulations of computational models become an interesting strategy towards studying relevant aspects on structural response of these members, despite the lack of experimental data. This study aims to propose a simple numerical model able to predict ultimate failure load of pGFRP angles connected by the leg using non-linear (geometrical and material) numerical analyses. Since the literature on pultruded angles connected by the leg are almost nonexistent, previous studies on steel angles [2–5] and pGFRP columns simulation are used as reference

to calibrate our model. Based on the literature review, parameters such as material properties and damage failure criteria, mesh size and shape, boundary and loading conditions, and others were evaluated and discussed.

2 Literature review

The mechanical behavior of angles connected by the leg have been studied on steel structures by many researchers [2–5]. The same is not true for composites profiles. There is a lack of information on pGFRP angles under eccentric compression and few researchers have addressed the problem of designing. To the best of the authors' knowledge, studies on bolted pGFRP angle members are limited to works developed by Selvaraj, Kulkarni and Babu [6], Godat et al. [7], Prasad Rao, Rokade and Balagopal [8], Balagopal, Prasad Rao and Rokade [9] and Monteiro and Malite [10]. Details of each paper can be found in Table 1.

Table 1. Studies on pGFRP angles including members connected by the leg

Paper	Experimental program						Theoretical analyses[7]	
		Tests with pGFRP angles						
		Specimen						
	Material properties[1]	Resin[2]	Nº	Slenderness b/t	Slenderness Global (minor axes)	Structural member[3]	Analytical	Numerical
Selvaraj, Kulkarni e Babu [6]	$E_{L,t}, F_{L,t}$ [1a]	E	NI[2]	8		IC	Euler	LBA (FE)
			24	8		Truss	Euler	LBA (FE)
Godat et al. [7]	$E_{L,t}, F_{L,t}$ [1a]	PO	6	12	75 e 100	IC	LBA	-
Prasad Rao, Rokade e Balagopal [8]	$E_{L,t}, F_{L,t}$ [1a]	PO	NI[4]	8	86 e 91	IC	-	NLBA (FE)
Balagopal, Prasad Rao e Rokade [9]	$E_{L,c}, F_{L,c}, G_{LT}$	NI[4]	12	12	40 a 100	IC	LBA	NLBA (FE)
			24	8 e 12		Truss	LBA + Design	NLBA (FE)
Monteiro and Malite [10]	V_f, G_{LT}, $F_{L,c}$, $E_{L,c}, E_{T,c}, E_{L,f}$	PO	24	8	29 a 136	IC	LBA + Design	-

[1]The properties required for theoretical analyses are listed. Fiber volume content (V_f), longitudinal modulus of elasticity and strength in compression $(E_{L,c}; F_{L,c})$, longitudinal modulus of elasticity and strength in flexure $(E_{L,f}; F_{L,f})$ e in-plane shear modulus(G_{LT}). [1a]The researchers considered an analogy between tensile and compression properties. Although they are not considered the most adequate solution, the properties are mentioned only so as not to omit information about the work methodology. [2] PO: Polyester; VI: Vinylester; E: Epoxy. [3]Isolated column.

As ca be noted from Table 1, the studies are focused on experimental investigation (although deficiencies are verified, particularly, in material characterization). Linear Buckling Analyses, referred to as LBA in Table 1, deals with the analytical procedure used to concentrically loaded columns (minimum value between Euler buckling load for flexural about the minor axis and flexural-torsional buckling load), i.e., ignoring eccentricity influence. Some works presented an even more simplified approach (referred to as Euler, in Table 1), where the resistance is directly associated with Euler's critical buckling load regardless of the failure mode.

Regarding numerical analyses, only Prasad Rao's group developed studies on FE simulations of pGFRP angles. In the first paper [8], the angle was modelled as an isolated member with loading directly applied in the model (without considering the presence of bolts or holes). In addition, the material properties used in the model were derived only from tensile coupon test. In the second article [9], the authors used mechanical properties obtained experimental tests, but the model remained similar to that used in the first paper. Based on the literature review it is clear that there is a need to address this significant knowledge gap.

3 Experimental program

This section reports the methods of an experimental investigation that assessed the eccentric compression behavior of pGFRP angle profiles of 50 × 6 mm nominal dimensions connected by the leg. The pGFRP material consisted of E-glass fibers, polyester resin, and calcium carbonate (filler) and the profile layout is comprised of UD roving in the core region and two outer Continuous Strand Mats (CSM).

Prior to column tests, material characterization — including mechanical (tensile, compression, flexural and in plane shear) and physical tests — was performed as presented in Monteiro and Malite [10]. Results from these tests that will be used as an input data of numerical model are presented in Section 4.2. Column tests allowed to assess buckling response and to obtain information about ultimate behavior of pGFRP angle members connected by the leg by two bolts. Four lengths (625, 775, 1075 and 1375 mm) were experimentally evaluated and tests were performed with two duplicate lengths' columns, totaling 8 specimens. Test setup configuration is shown in Fig. 1.

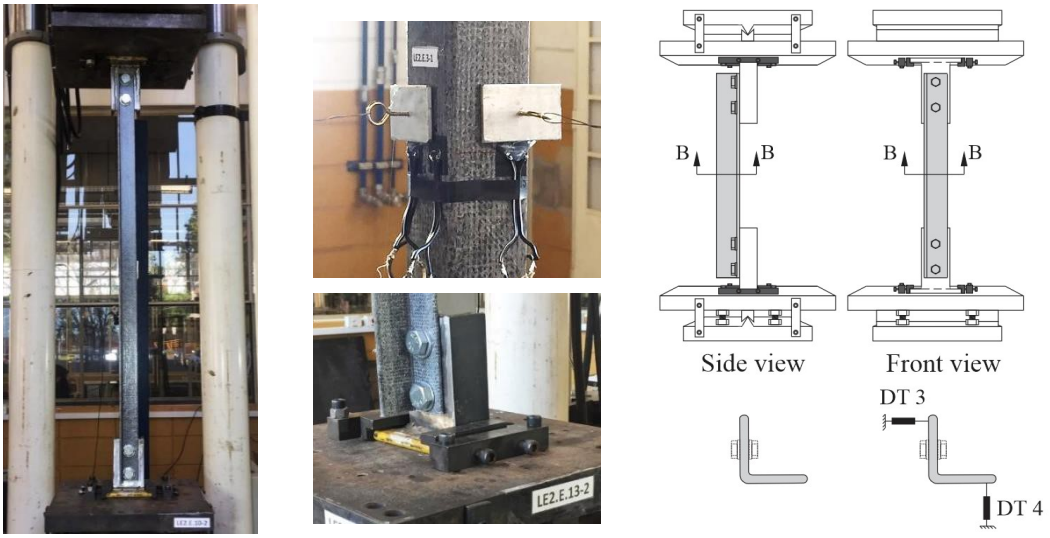

Figure 1. Experimental set up

The test setup proposed was designed simulating a typical framing connection used in practice. The ends of the angles were bolted to a device positioned on the testing machine so that the line of action of the load coincided with the bolt line. The device consisted of a steel U section with two 17-mm diameter holes, whose centers are 60 mm apart. It was fixed to the machine by an anti-slippage device. The connection system consisted of 5/8" A325 steel bolts and washers torqued to the finger-tightened condition. To measure lateral deflections, specimens were instrumented with two displacement transducers (DTs). All measurements were taken at mid-length. The tests were conducted in a model 8506 Instron servo-hydraulic universal testing machine of 2500 kN load capacity. Axial load was applied via displacement-controlled crosshead at a 0.3 mm/min rate up to failure.

4 Numerical analysis

This section describes the numerical study on the ultimate strength of pGFRP angles connected by the leg, which was conducted by using FE software ABAQUS® and involved eight 50 × 6 mm angle columns of four different lengths, namely 625, 775, 1075 and 1375 mm. This numerical study was based on works conducted by Branquinho and Malitte [3], Maia [4], Onésimo [2] and Paula [5] and validated with test results from experimental tests carried Monteiro and Malite [10] described in the previous section.

4.1 FE Model

The present study evaluates pGFRP angles connected by the leg by two bolts as an isolated member. The cross-section model dimensions and length assumed the average values measured. The wall thickness and width were 6.005 mm and 47.094 mm (midline dimension), respectively.

Towards representing the mechanical behavior of angles connected by the leg, two modelling approaches were adopted in the reference papers [2–5]: (i) three-part model [3] (angle member + support device + bolts) with application of loading in support devices (similarly to the experimental procedure shown in Figure 1); and (ii) one-part model [2,4,5] (only angle member) in which the load is directly applied on the angle and the presence of the screws is simulated through holes drilled in the model. In this paper, the last approach was adopted (Figure 2). Holes made in the angle's legs simulated the presence of the bolts.

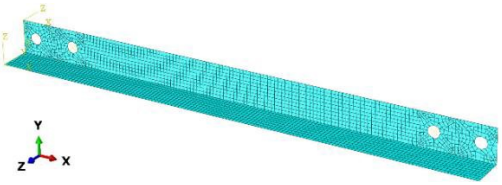

Figure 2. Finite element

4.2 Material properties and mesh

The pGFRP material was modelled as a transversally isotropic lamina defined by longitudinal (E_L = 28 GPa) and transverse (E_T = 8.32 GPa) moduli; major in-plane Poisson's ratio (ν_{LT} = 0.296 GPa); and in-plane (G_{LT} = 2.71 GPa) and interlaminar (G_{Ls} = G_{Ts} = 2.71 GPa) shear moduli. Longitudinal and in-plane shear modulus were obtained from experimental tests (three-point bending and Iosipescu (shear tests, respectively), whereas transverse modulus, Poisson's ratio and interlaminar shear modulus were determined analytically by mechanical models.

Since damage evaluation is important to accurately predict the ultimate load, material damage was considered through Hashin progressive damage model. The value of strength properties — tensile (X_t and Y_t), compression (X_c and Y_c) and shear strengths (X_s and Y_s) in the longitudinal (X) and transversal (Y) directions — and fracture energies (G) related to each failure mode used in this paper are shown in Table 1.

Table 1. Material properties

Strength (MPa)						**Fracture energy (N/mm)**			
X_t	X_c	Y_t	Y_c	S_{12}	S_{23}	$G_{f.t}$	$G_{f.c}$	$G_{m.t}$	$G_{m.c}$
476.27	497.93	41.45	43.34	45.98	45.98	23.7	23.7	8.9	8.9

Strength properties were obtained experimentally, whereas fracture energies were chosen based on numerical simulations performed considering values presented in literature. As experimental tests for obtaining fracture energy of pGFRP material is not yet standardized, alternative strategies have been used by researchers to define it. The fracture energy (G) in traction (subscript t) and compression (subscript c) in the direction of fibers (subscript f) and transverse to them (subscript m) reported literature on pGFRP members are indicated in Table 2.

Table 2. Fracture energies reported in literature

Paper	**Fracture energy (N/mm)**				**Viscosity**			
	$G_{f.t}$	$G_{f.c}$	$G_{m.t}$	$G_{m.c}$	$v_{f.t}$	$v_{f.c}$	$v_{m.t}$	$v_{m.c}$
Debski et al. [11]	133	10	0.5	1.6	5.10^{-4}	5.10^{-4}	5.10^{-4}	5.10^{-4}
Xin et al. [12]	12.5	12.5	1	1	5.10^{-4}	5.10^{-4}	5.10^{-4}	5.10^{-4}
Mendes [13]	23.7	23.7	8.9	8.9	10^{-5}	10^{-5}	10^{-5}	10^{-5}
D'aguiar [14]	2.38	5.28	0.424	0.95	10^{-5}	10^{-5}	10^{-5}	10^{-5}
Azevedo [15]	5	200, 100, 50, 5, 15	5, 10, 25, 50	70	10^{-5}	10^{-5}	10^{-5}	10^{-5}
Nunes et al. [16]	2.38	5.28	0.424	0.95	10^{-5}	10^{-5}	10^{-5}	10^{-5}
Regel et al. [17]	12.5	12.5	1	1	10^{-3}	10^{-3}	5.10^{-3}	5.10^{-3}

In fact, there is still no consensus in the scientific community regarding the fracture energies of the GFRP material [15]. Moreover, the literature is scarce and there is a high variability of the values in the few works available. After tests, values assumed by Mendes [13] were adopted. To improve the convergence of the numerical model and reduce the mesh dependence, a viscosity coefficient of 10^{-5} was used.

The widely adopted shell element S4R is used to discretize FE angle models. Numerical models with S4R5 and S4 shell elements were also evaluated before choosing S4R. The maximum difference among critical buckling load (P_{cr}) obtained by these shell element was 2,03%. To manage the computing source as well as accuracy, mesh convergence study was performed through eigenvalue buckling analyses. A quadrilateral mesh with element size 5 mm has been chosen. Tests with triangular mesh in the region of the holes were also performed, but no gain was observed in the results.

4.3 Boundary and load conditions

The reference papers [2–5] present some differences concerning boundary and load conditions, particularly with regard to displacements and rotations allowed and the length of the hole over which the loading was coupled. The assumptions adopted by each researcher is presented in Table 3. To evaluate the influence of these aspects on the proposed model, tests were performed assuming combinations of boundary and load conditions. Table 4 present the results of eigenvalue analyses in terms of P_{cr} obtained for LE2.13 (1375 mm) member.

Table 3. Boundary and load conditions adopted in the reference papers

Paper	Degree of freedom restrained (all hole)	Load application
Maia [4]	u_y,u_z	all hole, ½ hole and ¼ hole
Paula [5]	u_z,θ_x, θ_y, θ_z	"part with direct contact with screws"
Onésimo [2]	u_y,u_z, θ_x,	all hole

Table 4 shows tthat, except for Test 5, P_{cr} were reasonably close. The boundary and load conditions defined by Test 1 to Test 4 were chosen comparing P_{cr} obtained by numerical simulations of others specimens and their respectively P_{cr} predict by analytical equations based on Vlasov theory. Vlasov [18] proposed a system of three differential equations for eccentrically compressed columns. Since Vlasov theory was originally developed and used for metallic elements, in this paper the formulation is used as an extension. Details of the Vlasov formulation used in this paper can be found in Onésimo [3].

Table 4. Boundary and load conditions numerical tests

Test	Degree of freedom restrained (all hole)	Load application	Critical buckling load - P_{cr} (kN)
1	u_y,u_z	¼ hole	16,935
2	u_y,u_z	½ hole	17,031
3	u_y,u_z, θ_x,	¼ hole	18,593
4	u_y,u_z, θ_x,	½ hole	18,649
5	u_y,u_z, θ_x,	all hole	8,019

Fig. 3 shows P_{cr} results obtained through numerical analyses performed with LE2.10 (1075 mm), LE2.7 (1075 mm) and LE2.6 (625 mm) columns and considering load and boundary condition Nº 1. In Fig. 3, slenderness ratios are given by k_zL_z/r_z, where k_zL_z and r_z are the effective length for flexural and radius of gyration about minor z axis, respectively. The red and blue lines in Fig. 3 refer to P_{cr} predicted through Vlasov's equation assuming: k_x = 0.5 and k_x = 1, respectively, where x axis is the longitudinal axis. In this study, k_z and k_y (y is the major axis) was assumed equal to 0.5 and the column ends were attributed to the center of connections. Fig. 3shows that boundary and loading condition Nº 1 enabled an adequate prediction of the critical buckling load.

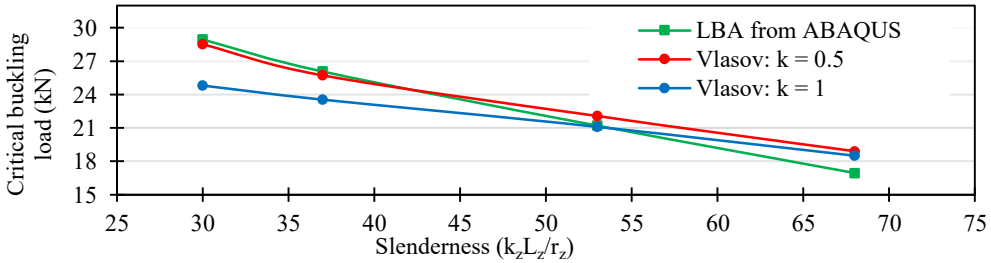

Figure 3. Critical buckling load obtained by FE model and Vlasov equation

4.4 Numerical analyses and validation

Numerical simulations were made for both linear and non-linear analyses. At the first step of modeling, by using eigenvalue analyses, the critical buckling loads are obtained for the first mode. At the second step, for non-linear analyses (NLA), the ultimate loads were obtained using the modified Riks method with arc-length control. For NLA, the numerical model considers material nonlinearity as presented in 4.2. Regarding initial geometric

imperfections, they were not considered in our model. As Maia [4] and Branquinho and Malite [3] observed, such imperfections exert a marginal effect on the angle strength, since their amplitudes are in general insignificant compared to the eccentricity imposed by the leg. Onésimo [2] also assumed this type of imperfection as negligible.

Model validation considered the verification of both linear (critical buckling load) and non-linear (ultimate failure load) results. Critical buckling load was compared to predictions obtained through Vlasov theory, as shown in Fig. 3. The ultimate failure loads were compared to the experimental results from Monteiro and Malite [10] (8 L50 × 6 mm angles). Fig. 4 shows a comparison of the numerical (proposed model) and experimental load (P) vs. displacement (D) for LE2.13.1 and LE2.13.2 members (1375 mm).

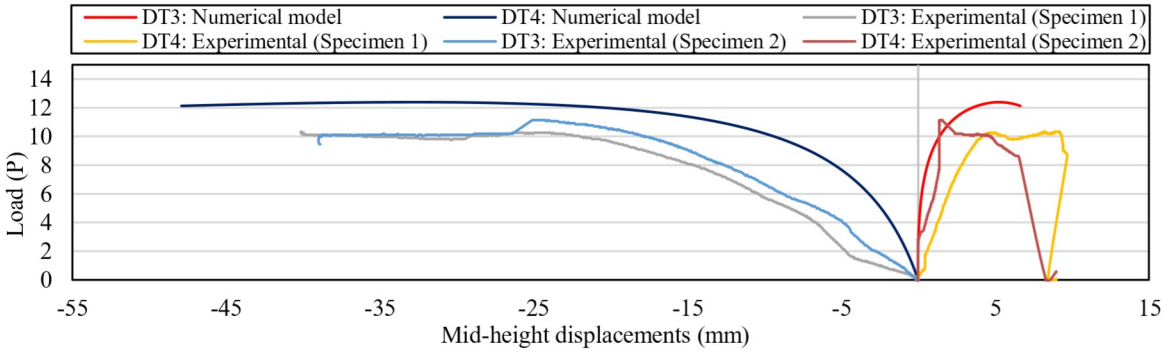

Figure 4. Load (P) vs. displacement (D) for LE2.13.1 and LE2.13.2: numerical and experimental results

In Fig. 4, P is the load applied along the column through the leg and DT3 and DT4 are the displacements in the DT3 and DT4 (transducers directions, respectively (see Fig. 1). As the main objective of the model proposed is to predicted ultimate load P_u, according to the Fig.4, it is possible to conclude that there is an acceptable consistency between numerical and experimental results. Comparison of the P_u obtained by experimental tests and numerical simulation for other angle members are presented in the next section (Table 5).

Besides eccentric compression analyses presented here, additional preliminary studies had been developed with members under concentric compression and the P_{cr} had been verified through analytical formulations.

4.5 Comparison between experimental and theoretical results

Table 5 presents P_{cr} obtained by both analytical (concentrically and eccentrically loaded columns) techniques, as well as their comparisons with eigenvalue predictions for FE model. Based on Linear Buckling Analyses (LBA) for angles under concentric compression, P_{cr} is given by the minimum value between Euler buckling load for flexural about the minor axis (P_{crz}) and flexural-torsional buckling load (P_{crFT}). To include eccentricity in problem, Vlasov equation as presented by Onésimo [3] was used. LBA by FE was performed as described previously. The observation of these results prompts the following remarks: (i) neglecting eccentricity overestimated the analytical results by up to 37.5%; (ii) a good agreement was found in prediction given by Vlasov and numerical LBA.

Table 5. Experimental critical (P_{cr}) and ultimate loads (P_u)

ID	$k_z L_z/r_z$	Analytical (P_{cr}): LBA (k = 0,5)		Experimental (P_u)		Numerical: FE	
		Concentrically loaded mín{P_{crz},P_{crFT}}	Eccentrically loaded (Eq.1)	L1	L2	LBA (P_{cr})	NLBA (P_u)
LE2.6	30	30,509	28,502	21,256	24,701	28,935	29,049
LE2.7	37	28,455	25,713	19,277	-	26,058	24,465
LE2.10	53	26,713	22,061	12,900	13,707	21,193	16,949
LE2.13	68	25,982	18,894	10,335	11,141	16,935	12,139

Ultimate load (P_u) obtained from experiments for replicated specimens L1 and L2 are also reported in Table 5. Except for LE2.6 column, Nonlinear Buckling Analyses (NLBA) approach obtained by FE analyses provided better estimations. This result shows that the current procedures in which eccentricity is neglect and/or pGFRP member are dimensioned as perfect columns [6-8] not provide an accurate estimate. For LE2.6, the numerical model seems to indicate a reserve of strength that is not observed experimentally. Although, NLBA model had provided the best agreement with experimental results among the methods evaluated in this paper, the model error still needs to be reduced. Advances in damage propagation analyses should contribute in this regard.

5 Conclusion

This paper has addressed a numerical investigation on the mechanical behavior of a pultruded Glass Fiber Reinforced Polymer (pGFRP) angle columns eccentrically loaded. The numerical model was calibrated according to analytical prediction experimental results from eight 50×6 mm pGFRP angles connected by the leg by two bolts. The main conclusions are summarized in what follows.

A one-part model, i.e., a model considering only the bar (without bolts and other devices) seems to be sufficient to predict the critical buckling load and ultimate load of angles connected by the leg satisfactory. With regard to the eigenvalue and non-linear analyses using the Finite Element (FE) method, it is possible to point that: (i) the difference between the critical buckling loads obtained from Vlasov equation and the numerical model was considered satisfactory; and (ii) numerical model including geometrical and material nonlinearities provide better agreement with experimental results when compared to the other predictions approaches evaluated in this paper.

Acknowledgements. This study was financed in part by the Coordenação de Aperfeiçoamento de Pessoal de Nível Superior - Brasil (CAPES) – Finance Code 001, and the National Council for Scientific and Technological Development, CNPq, (Process number 141880/2020-1).

Authorship statement. The authors hereby confirm that they are the sole liable persons responsible for the authorship of this work, and that all material that has been herein included as part of the present paper is either the property (and authorship) of the authors, or has the permission of the owners to be included here.

References

[1] T. V Galambos, Guide to stability design criteria for metal structures, 5th ed., John Wiley & Sons, Inc, 1998.
[2] J. Onésimo, G. Junyor, H. Carvalho, A.C. Campos, Análise teórico-numérica da influência do número de parafusos no comportamento de cantoneiras laminadas comprimidas concêntrica e excentricamente, 9 (2020) 21–40.
[3] M.Á. Branquinho, M. Malite, Effective slenderness ratio approach for thin-walled angle columns connected by the leg, J. Constr. Steel Res. 176 (2021).
[4] W.F. Maia, Sobre a estabilidade de cantoneiras de aço formadas a frio à compressão, Escola de Engenharia de São Carlos, EESC-USP, 2008.
[5] V.F. de Paula, Análise Numérica de Cantoneiras de Aço Formadas a Frio, Sob Tração e Conectadas por Parafusos, Universidade de Brasília, 2017.
[6] M. Selvaraj, S.M. Kulkarni, R.R. Babu, Behavioral Analysis of built up transmission line tower from FRP pultruded sections, Int. J. Emerg. Technol. Adv. Eng. 2 (2012).
[7] A. Godat, F. Légeron, V. Gagné, B. Marmion, Use of FRP pultruded members for electricity transmission towers, Compos. Struct. 105 (2013) 408–421.
[8] N. Prasad Rao, R.P. Rokade, R. Balagopal, Failure investigation of GFRP communication towers, Eng. Fail. Anal. 79 (2017) 397–407.
[9] R. Balagopal, N. Prasad Rao, R.P. Rokade, Investigation on Buckling Behaviour of GFRP Angle Sections with Bolted Connections in Lattice Towers, J. Inst. Eng. Ser. A. (2020).
[10] A.C.L. Monteiro, M. Malite, Behavior and design of concentric and eccentrically loaded pultruded GFRP angle columns, Thin-Walled Struct. 161 (2021) 107428
[11] H. Debski, P. Rozylo, A. Teter, Buckling and limit states of thin-walled composite columns under eccentric load, Thin-Walled Struct. 149 (2020) 106627.
[12] H. Xin, A.S. Mosallam, Y. Liu, C. Wang, J. He, Experimental and numerical investigation on assessing local bearing behavior of a pultruded GFRP bridge deck, Compos. Struct. 204 (2018) 712–730.
[13] J.D.R.S. Mendes, Comportamento mecânico de ligações aparafusadas em materiais FRP, Instituto Superior Técnico, Universidade Técnica de Lisboa, 2017.
[14] S.C.M. D'Aguiar, Estabilidade de colunas de material compósito reforçado por fibras, Universidade Federal do Ceará, 2017.
[15] J.P.S.V.S. de Azevedo, Contributo para o desenvolvimento de um sistema inovador de ligação entre perfis de compósito de GFRP, Técnico Lisboa, 2016.
[16] F. Nunes, N. Silvestre, J.R. Correia, Structural behaviour of hybrid FRP pultruded columns. Part 2: Numerical study, Compos. Struct. 139 (2016) 304–319. https://doi.org/10.1016/j.compstruct.2015.12.059.
[17] F. Regel, F.W.J. Van Hattum, G.R. Dias, A numerical and experimental study of the material properties determining the crushing behaviour of pultruded GFRP profiles under lateral compression, J. Compos. Mater. 47 (2013) 1749–1764.
[18] V.Z. VLASOV, Pieces Longues en Voiles Minces, Trad. G. Smirnoff. Paris, Eyr (1962).